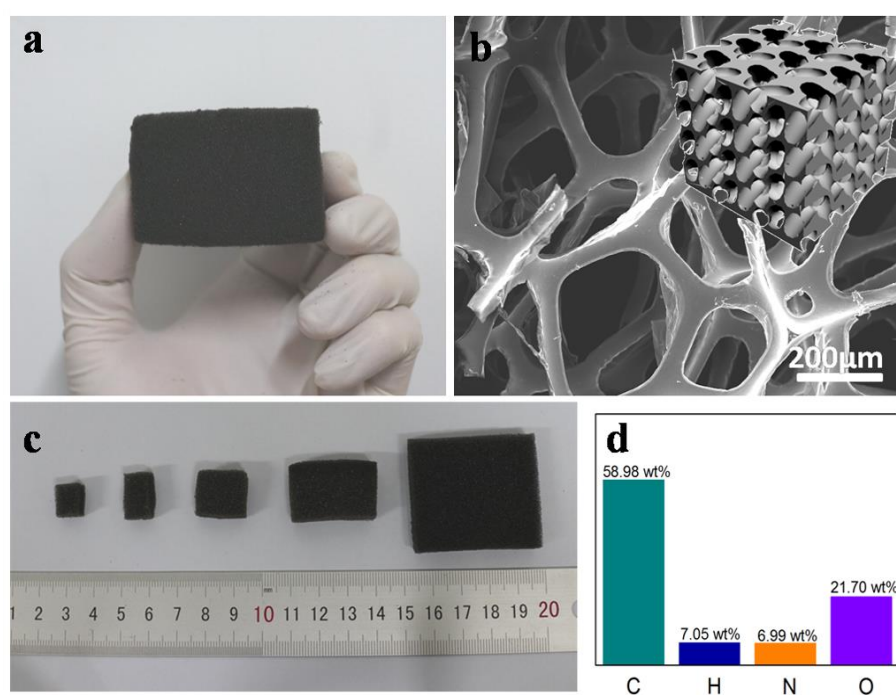


## Supporting Information

### Facile and Generalized Encapsulations of Inorganic Nanocrystals with Nitrogen-doped Carbonaceous Coating for Multifunctionality

Yong Yang, Jingchao Zhang, Shitong Wang, Xiaobin Xu, Zhicheng Zhang, Pengpeng Wang, Zilong Tang, Xun Wang\*



**Figure S1.** a) A typical photo image of commercial PU sponge. b) SEM image of PU sponge. the inset is the model of commercial PU sponge. c) Photograph of small PU cubes with different weight. d) Chart showing the percentages of C, H, N and O in the commercial PU sponge measured by elemental analysis system.

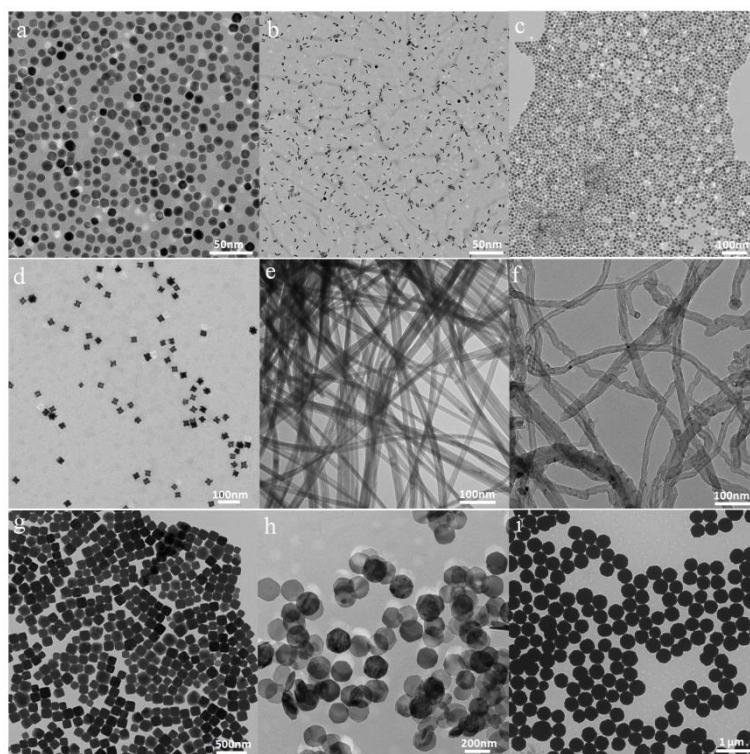


**Figure S2.** TEM images of nanocrystals. Au nanoparticles ( $7\pm 1$  nm) (a); Au nanorods ( $50\pm 5$  nm) (b); Pd nanocubes ( $8\pm 1$  nm) (c); Pt nanocubes ( $20\pm 3$  nm) (d);  $\text{MnO}_2$  nanowires (e); CNTs (f), Prussian blue nanocubes ( $120\pm 10$  nm) (g);  $\text{Fe}_2\text{O}_3$  nanoplates ( $150\pm 10$  nm) (h); CdS nanoparticles ( $250\pm 10$  nm) (i).

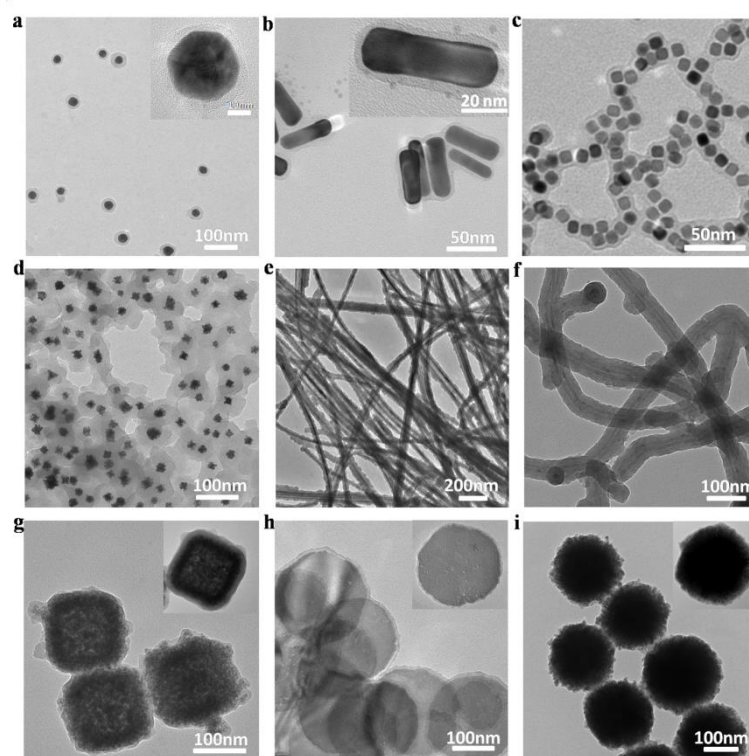


**Figure S3.** TEM images of nanocrystals with N-doped carbonaceous coating. a) AuNPs/N-C; b) Au nanorods/N-C; c) Pd nanocubes/N-C; d) Pt concaves/N-C; e) MnO<sub>2</sub> nanowires/N-C; f) CNTs/N-C; g) Fe<sub>2</sub>O<sub>3</sub> nanoboxes/N-C; h) Fe<sub>2</sub>O<sub>3</sub> nanoplates/N-C; i) CdS nanospheres/N-C. The inset represents typical enlarged TEM images.

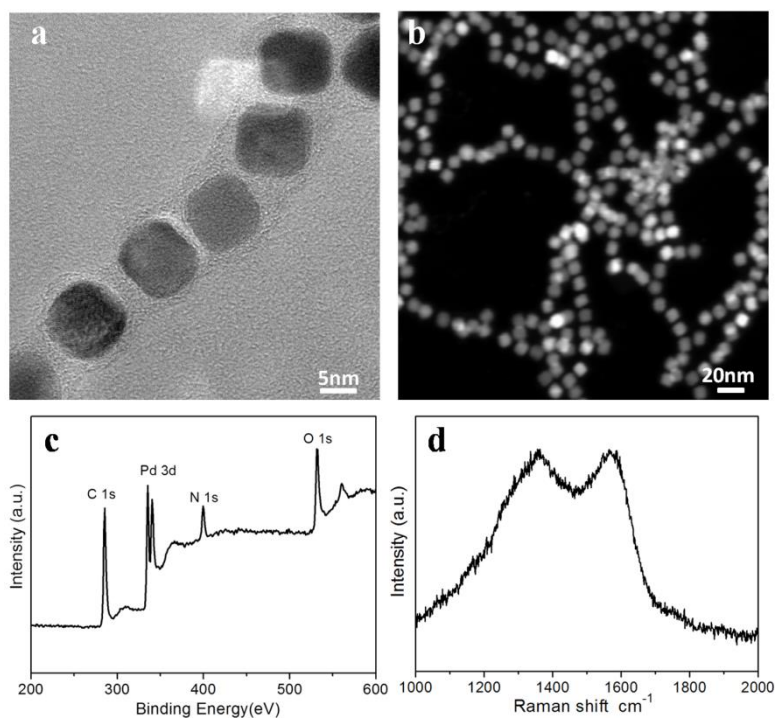


**Figure S4.** a-b) HRTEM and STEM images of Pd/N-C structure. c) XPS spectra of Pd/N-C. d) Raman spectrum of the Pd/N-C.

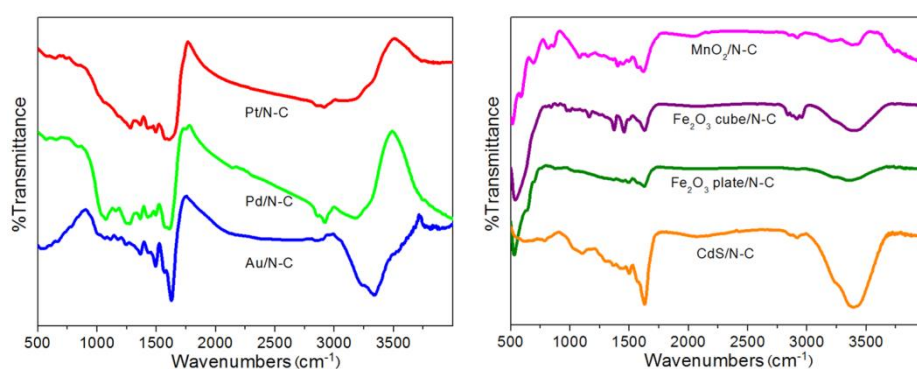


**Figure S5.** Fourier transform infrared (FT-IR) spectra of hybrid composites

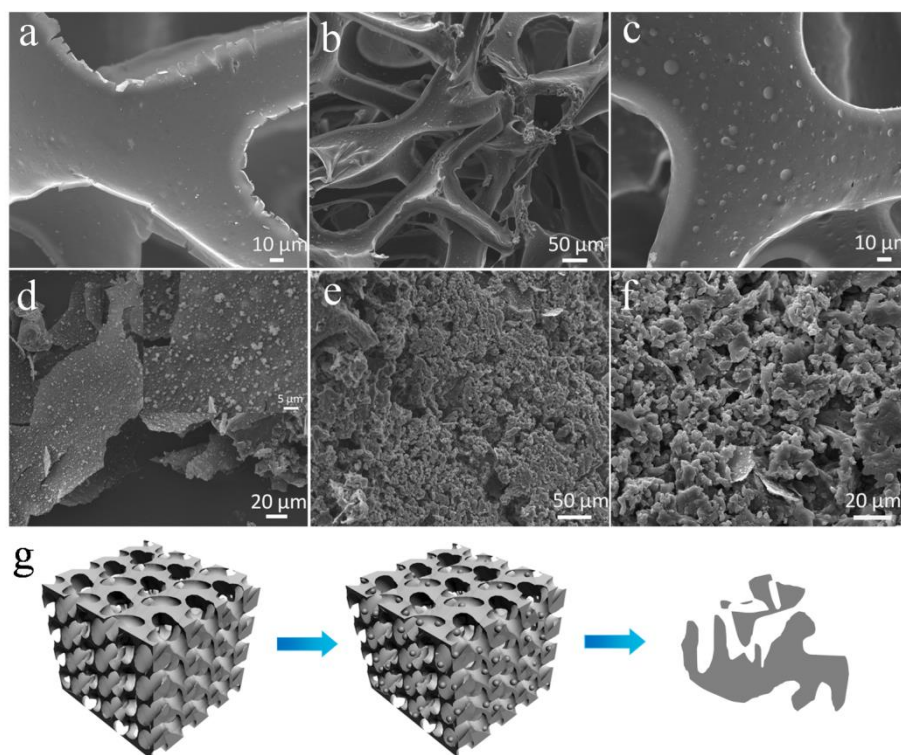


**Figure S6.** (a) SEM image of pristine PU sponge. SEM images of PU sponge during the hydrothermal treatment at 200 °C with different reaction time: b-c) 2 h; d) 6 h; e-f) 12 h. g) Schematic illustration of the evolution of PU sponge under hydrothermal treatment.

**Table S1.** XPS analysis of of the PU sponge before and after hydrothermal treatment

	Raw PU sponge (%)	The final product after hydrothermal treatment (%)
C atoms	68.24	71.77
N atoms	6.06	1.41
O atoms	25.7	26.82

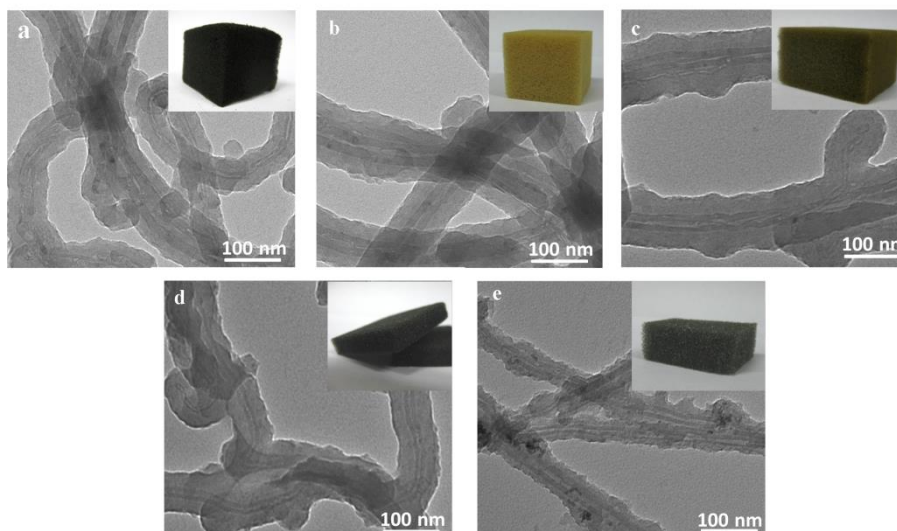


**Figure S7.** TEM images of CNTs/N-C synthesized by hydrothermal treatment with various PU sponges at 200°C for 2 hours. The inset is the corresponding picture PU precursors.

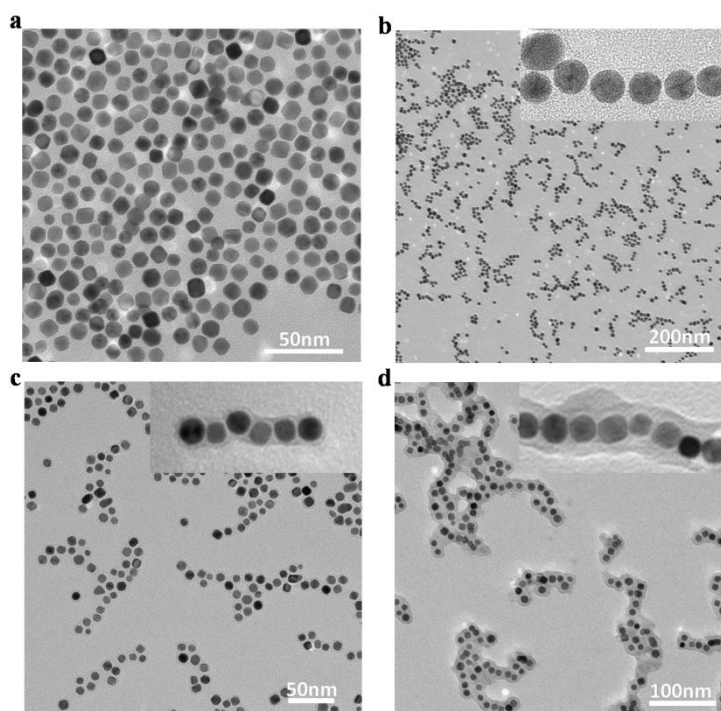


**Figure S8.** TEM images of 8-nm-diameter Au/N-C composite synthesized at 200°C under different reaction time. a) 0 min; b) 40min; c) 80min; d) 120min. The inset is the corresponding enlarged image, indicating the coating thickness gradually increases over time.

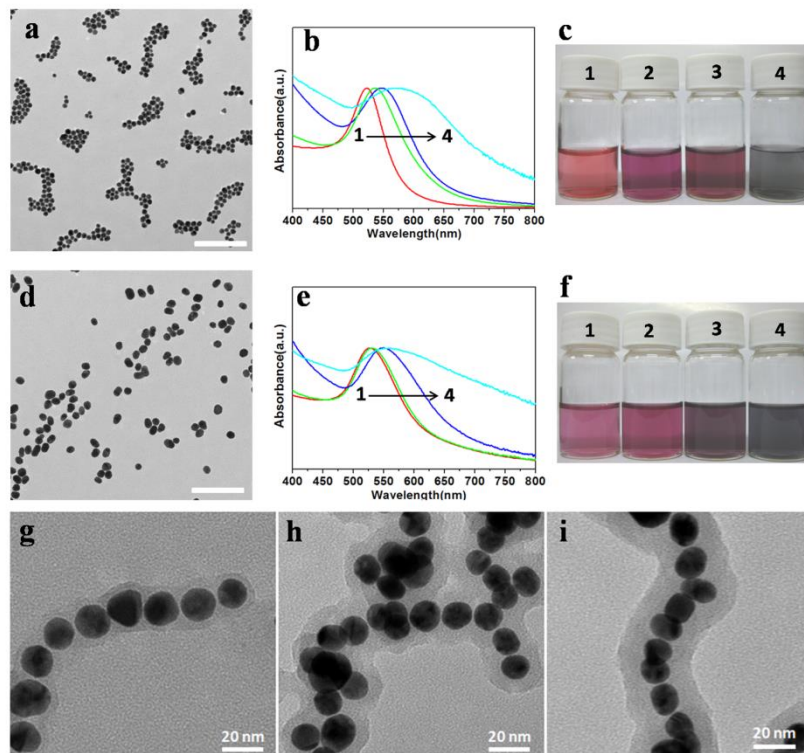


**Figure S9.** a,d) TEM images of 18-nm-diameter and 28-nm-diameter AuNPs. Scale bars: 100nm. b,e) UV-vis extinction spectra and the color change of 18-nm-diameter Au/N-C composite under different time from left to right, 0 min; 40min; 80min; 120min. c,f) UV-vis extinction spectra and the color change of 28-nm-diameter Au/N-C composite under different time from left to right, 0 min; 40min; 80min; 120min. g-i) TEM images of 18-nm-diameter Au/N-C composite obtained by changing the amount of PU sponge after hydrothermal treatment for 3h.

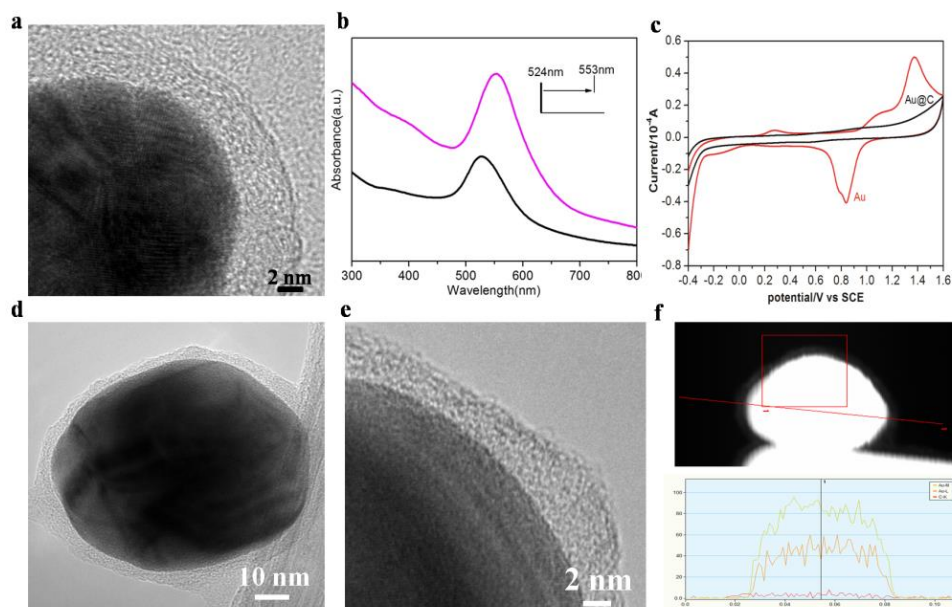


**Figure S10.** a) HRTEM image of 28-nm-diameter AuNPs/N-C. (b) The absorbance spectrum of aqueous 28-nm-diameter AuNPs (black) before and after coating (purple). Note that the UV-vis spectra of AuNPs displays a characteristic absorbance at 524 nm. However, there was a red-shifted absorbance spectrum at 553 nm after coating. c) CV curves of bared AuNPs (red) and AuNPs/N-C composites (black) on glassy carbon electrodes in 0.5 M H<sub>2</sub>SO<sub>4</sub> solution. Scan rate: 100 mV/s. d-e) TEM and HRTEM imag of 55-nm-diameter Au/N-C on carbon nanotube grid. f) STEM image of typical Au/N-C and cross-sectional compositional line profiles.

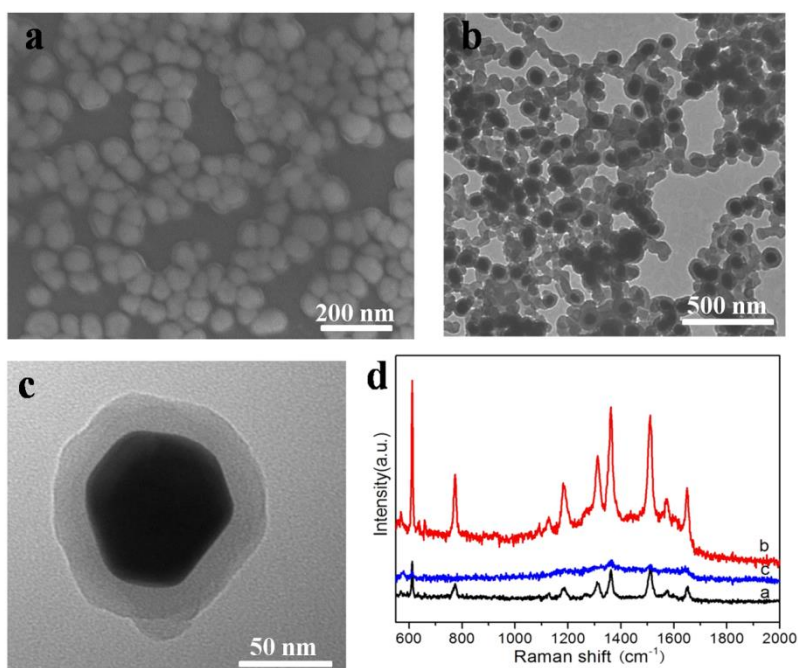


**Figure S11.** a) Typical TEM image of 55-nm-diameter Au/N-C. b-c) SEM images of 55-nm-diameter Au/N-C of ca. 10 nm shell. d) SERS spectra of 10<sup>-7</sup> M R6G adsorbed on the pure AuNPs at 633 nm laser excitation (a, black), Au/N-C of ca. 2 nm shell (b, red) and Au/N-C of ca. 10nm shell (c, blue).

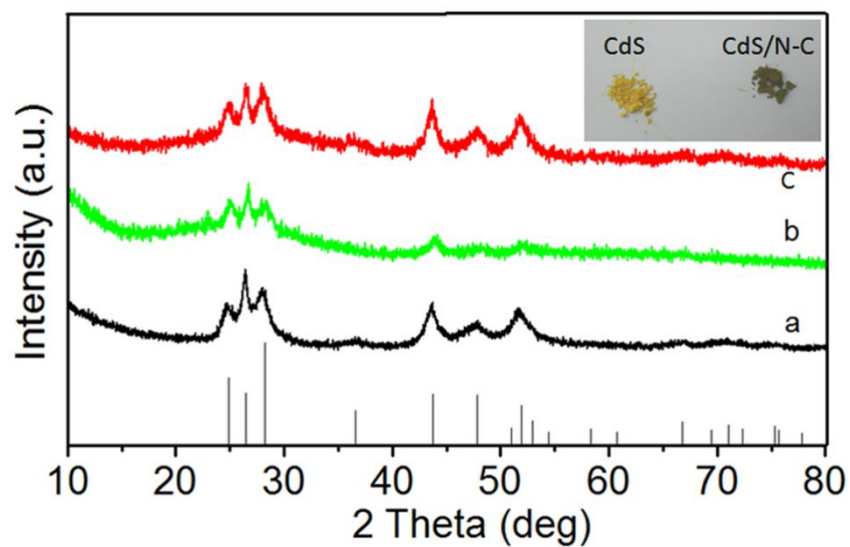


**Figure S12.** A) XRD patterns of pure CdS (a); CdS/N-C hybrid composites (b); CdS/N-C hybrid composites calcined in air at 450 °C for 30 minutes (c). The inset represents the color of CdS before and after coating.

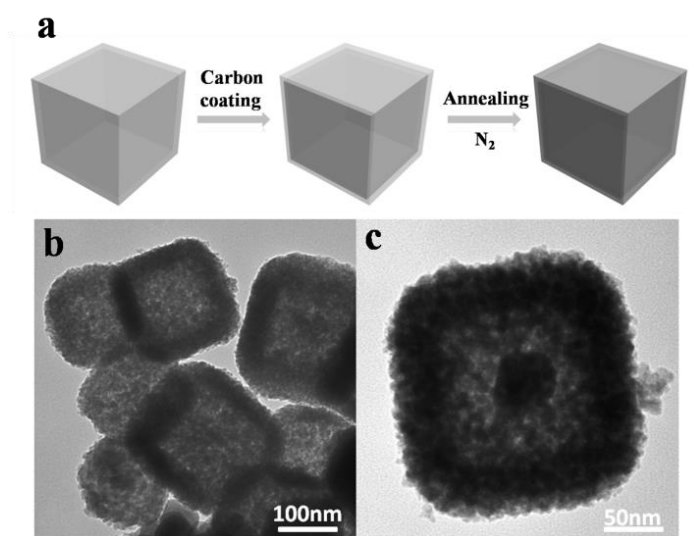


**Figure S13.** a) Schematic illustration for the formation of  $Fe_2O_3$ /N-C nanoboxes with N-doped carbonaceous coating. b-c) TEM images of the as-prepared  $Fe_2O_3$  nanoboxes under different magnifications.



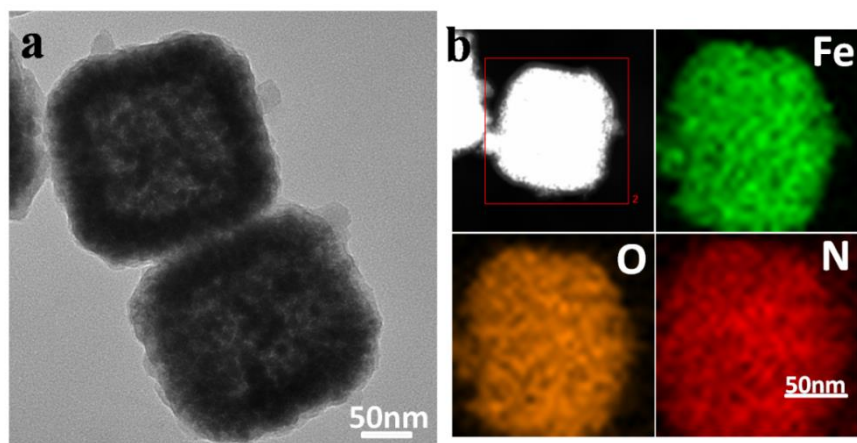


**Figure S14.** a) TEM image of the as-prepared  $\text{Fe}_2\text{O}_3/\text{N-C}$  nanoboxes. (b) EDS mapping images of  $\text{Fe}_2\text{O}_3/\text{N-C}$ .

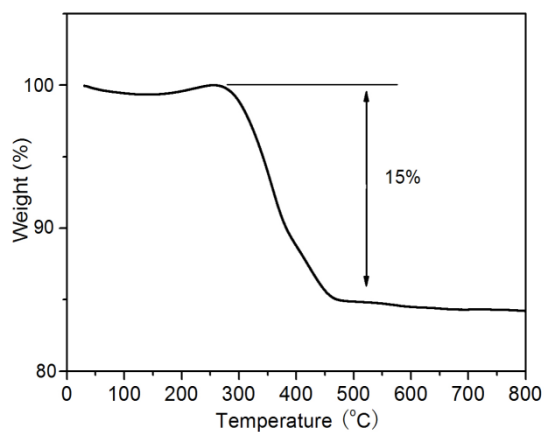


**Figure S15.** TGA curve of  $\text{Fe}_2\text{O}_3/\text{N-C}$  nanoboxes in air flow, indicating that composites contain 15 wt% of carbon.

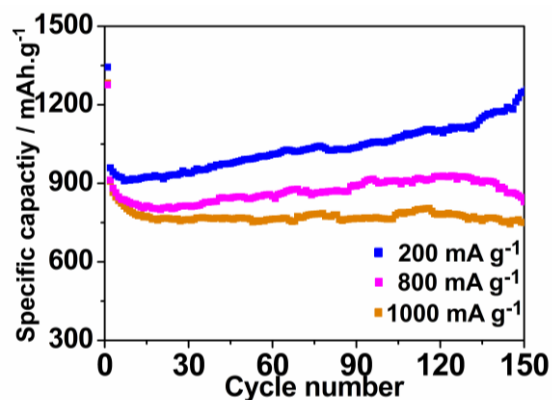


**Figure S16.** Cycling performance of  $\text{Fe}_2\text{O}_3/\text{N-C}$  with different current densities between 0.01 and 3.0 V.